International Journal of Applied Chemistry.
ISSN 0973-1792 Volume 13, Number 4 (2017) pp. 855-877

http://www.ripublication.com

Kinetic Analysis of Thermal Degradation of Poly (Vinyl Alcohol)/Starch/Nano Clay Nanocomposite Using Differential Isoconversional and Master Plot Approaches

Esmat Sedaghat[1]*, Abbas Ali Rostami[2], Mousa. Ghaemy[3], Ali Rostami[4]

[1,2,3]Faculty of Chemistry, University of Mazandaran, P. O. Box 453, Babolsar, Iran
[4]Faculty of Science, Department of Chemistry, Shahid Beheshti University, Evin, Tehran, Iran
***Correspondence:** Esmat Sedaghat, Babolsar, Iran,*

Abstract:

Starch/poly (vinyl alcohol) (PVA) blends and starch/PVA/montmorillonite (MMT) nanocomposites were prepared at various ratios via solution casting method in order to overcome the common drawbacks of pure starch films. The microstructural observations by FESEM revealed that the MMT was well dispersed into polymer matrix homogeneously. Thermal degradation of PVA/starch blends and PVA/starch/MMT nanocomposites by thermogravimetric analysis (TGA) under non-isothermal conditions indicated four stages of weight reduction. Kinetic analysis of the non-isothermal degradation of starch/PVA blends and starch/PVA/MMT nanocomposites was performed using isoconversional (Flynn-Wall-Ozawa, Kissinger-Akahira-Sunose and Friedman) methods and the invariant kinetic parameters method. The dependence of conversion (α) on the temperature and activation energy was determined allowing the calculation of master plots. The experimental master plots agreed with the nucleation and growth kinetic function for starch/PVA blends and starch/PVA/MMT nanocomposite. The biodegradability of the blend and nanocomposite films was investigated based on burial in soil and compost. Dynamic and mechanical thermal analysis (DMTA) was used in order to assess the effectiveness of MMT on the final mechanical properties of the prepared nanocomposite.

Keywords: Master plot analysis; Nanocomposite; biodegradability; Kinetic analysis; Thermal degradation

1. INTRODUCTION

Nanocomposites are a new class of hybrid materials composed of nanofiller incorporated into a based matrix [1]. Such an association between eco-friendly polymers and nano-objects is one of the most innovating routes to rise the of these matrices [2].

In recent decades, a significant endeavor has been devoted to the development of polymer−clay nanocomposites. These materials with a low cost and a vast range of potential technological applications have attracted a great deal of interest in both industrial and academic areas, with new issue rising every year [3−12]. After cellulose, starch is considered as the most plentiful natural biopolymer [13]. It is also especially attractive due to its biodegradability and low cost [14]. It also has the ability to form films that are odorless, colorless, transparent, and with very low oxygen permeability [15]. But there are disadvantages such as poor mechanical properties; highly hydrophilic properties in nature and poor water barrier properties.

Several studies have shown that adding polar synthetic polymers such as Poly (vinyl alcohol) (PVA) to starch improves the physical and mechanical properties of films obtained [16]. The formation of hydrogen bonds between the hydroxyl groups on the starch and polyvinyl alcohol could increase potentially the capability of miscibility and improve the physical and mechanical properties of their blends [17-19]. PVA/thermoplastic starch blends show a broad range of physical properties and other advantageous characteristics and can be employed in a wide range of applications. To further improve their characteristics, some physical and chemical methods such as crosslinking, incorporation of nanoparticles can be applied [20-23]. The incorporation of clay fillers into the polymer matrices improves their thermal stability.

There are reports of studies of thermal stability (degradation) of PVA/starch/organically modified MMT [24] and polystyrene/MMT nanocomposite [25]. Susmita et al. studied thermal stability of PVA/starch films by using organically modified MMTs [24]. Vyazovkin et al. [25] reported the thermal stability of polystyrene/clay nanocomposite. They showed that PS/clay nanocomposites have 30-40 °C higher degradation temperature compared to pure PS under nitrogen and air heating degradation conditions. Also, Fakhrpour et al. [26] and Erceg et al. [27] studied degradation kinetics of PET/PEN blend and poly (3-hydroxybutyrate) nanocomposites using differential isoconversional/ master plot approaches and non-isothermal degradation, respectively.

In this study, some aspects concerning the thermal decomposition of starch/PVA/MMT nanocomposites with different percentages of nanoclay prepared

by casting method were studied. The aim of this work was to investigate the thermal decomposition behavior of PVA/starch blend and PVA/Starch/clay nanocomposites. Thermal analysis of the mixtures was performed by TG/DTG under dynamic conditions. The activation energy (Eα) of the non-isothermal degradation was determined by various Isoconversional methods: Flynn-Wall-Ozawa (FWO) [28, 29], Kissinger-Akahira-Sunose (KAS) [30, 31] and Friedman (FR) methods. Isoconversional methods yielded the effective activation energy (Ea) as a function of the extent of conversion (α).

1.1. Theoretical background

The kinetic parameters of a thermal decomposition reaction can be evaluated by dynamic experiments. In this case, the sample is heated from room temperature until its complete decomposition at a linearly programmed rate. The TGA technique is feasible for monitoring the weight loss of a material during a heating process. Primarily to determine the kinetic parameters, the degree of conversion (α) must be obtained. The value of α can be determined in terms of mass loss from the TG curves as follows:

$$\alpha = \frac{m_0 - m}{m_0 - m_\infty} \tag{1}$$

Where m is the measured mass of sample at temperature T, m_o is the initial mass, and m_∞ is the mass at the end of the non-isothermal TGA experiment. The rate of conversion for a solid-state reaction is commonly assumed as the product of two functions: One function pertains just on the temperature T and the other just on the fraction that is transformed as:

$$\frac{d\alpha}{dt} = k(T)f(\alpha) \tag{2}$$

$$f(\alpha) = (1 - \alpha)^n \tag{3}$$

Where α is a degree of conversion, $f(\alpha)$ the conversion function (reaction model). Most commonly form of $f(\alpha)$ for solid state reactions is $(1-\alpha)^n$ and "n" is the reaction order. The logarithm of Eq.3 results the following expressions:

$$-\ln(1-\alpha) = \mathrm{kT} + \mathrm{C} \tag{4}$$

The plot of $-ln(1-\alpha)$ versus T gives a straight line with a slope of k which is defined as the rate constant dependence to activation energy and can be expressed

according to the following Arrhenius equation:

$$k(T) = Aexp(-\frac{E_\alpha}{RT}) \quad (5)$$

Where E_α is the apparent activation energy, A is the pre-exponential factor, T is the absolute temperature, and R is the gas constant. The combination of Eqs. (2) and (5) provides the following relationship:

$$\frac{d\alpha}{dt} = Aexp(-\frac{E_\alpha}{RT})f(\alpha) \quad (6)$$

If the sample temperature is changed with a controlled heating rate, $\beta = dT/dt$, the variation in the degree of conversion can be analyzed as a function of temperature which depends on the time of heating. Hence, the reaction rate may be shown as:

$$\frac{d\alpha}{dt} = \frac{d\alpha}{dT}\frac{dT}{dt} = \beta\frac{d\alpha}{dT} \quad (7)$$

Where da/dT is the non-isothermal reaction rate, da/dt is the isothermal reaction rate, and dT/dt is the heating rate (β). Substituting Eq. (6) into Eq. (7) gives:

$$\frac{d\alpha}{dT} = \frac{A}{\beta}exp(-\frac{E_\alpha}{RT})f(\alpha) \quad (8)$$

The conversion dependence of the process rate can be expressed by using a wide variety of reaction models, $f(\alpha)$, some of which are shown in Table 1 [32].

To obtain the activation energy, several differential methods as well as integral methods have been developed. The Kissinger method is self-determining of any pre-supposition about the thermal degradation mechanism. This method relates the logarithm of $\frac{\beta}{T_p 2}$ with the inverse of the peak temperature by the following expression:

$$-ln(\frac{\beta}{T_P^2}) = \frac{E_\alpha}{RT_P} - ln(\frac{AR}{E_\alpha}) \quad (9)$$

Plotting $-ln\ (\frac{\beta}{T_p 2})$ versus $1/T_p$ gives a straight line from which the activation energy and pre- exponential factor can be determined from the slope and intercept of the plot, respectively. Flynn-Wall-Ozawa (FWO) method is a linear integral method based on Eq. (10):

$$log\beta = log\frac{AE}{Rg(\alpha)} - 2.315 - 0.4567\frac{E}{RT} \quad (10)$$

Plotting log β versus *1/T* gives a straight line from which the activation energy can be determined from the slope of the plot. Model-free isoconversional methods are based on the analysis of multiple TGA curves obtained at different heating rates and assume that the degradation function f(α) does not change with the heating rate for all values of α [33]. Therefore, the activation energy of the degradation process can be clearly estimated as a function of the extent of conversion. Isoconversional methods usually give more accurate values for the activation energy. Friedman's isoconversional method [34, 35] is a differential algorithm. This method is based on the logarithm of Equation (8):

$$ln\left[\beta_i\left(\frac{d\alpha}{dt}\right)_{\alpha,i}\right] = ln\left[A_\alpha f(\alpha)i\right] - \frac{E_{\alpha,i}}{RT_{\alpha,i}} \qquad (11)$$

Where subscripts *i* and α determine a given value of heating rate and extent of conversion, respectively. A plot of ln [β(da/dT)] versus *1/T* from thermograms recorded at several heating rates, should be a straight line whose slope allows the calculation of the activation energy. Invariant kinetic parameters (IKP) method [36] is based on the existence of the linear compensation effect (Eq. (12)) between *E* and *lnA* obtained for the same TGA curve by various theoretical kinetic models:

$$lnA = a^* + b^* E \qquad (12)$$

Where *a** and *b** are the compensation effect parameters. Also, the most generally used methodologies about the kinetic function, *f(α)*, which allows the comparison of the experimental to theoretical master-curves. Master curves are the reference theoretical plots which depend on the kinetic models, but normally are independent of the kinetic parameters of the process. As the experimental kinetic data could be transformed to the experimental master curves, comparison of the theoretical master curves with the experimental data allows selecting the appropriate kinetic model or, at least, the type of appropriate kinetic algorithm. [37-38].

2. EXPERIMENTAL

2.1. Materials

The Starch (St) used in this study was soluble extra pure. Starch was purchased from Merck Co. Its molecular weight is 342.30 g.mol^{-1}, pH= 6.0 - 7.5 (20 g/l, H_2O, 25 °C) and the bulk density is 300 kg/m^3. Poly vinyl alcohol (PVA) with M_n= 49000 was obtained from Fluka Co. Glycerol (M_n = 92.10, grade of pure 85%), as starch plasticizer, was provided by Fluka Chemical Co. Montmorillonite (MMT) KSF with Molecular Weight 294.19 was kindly supplied by Aldrich Chemical Co and its chemical formula is Al2O3·2SiO2·2H2O. The water used to prepare starch/polyvinyl alcohol blend films was distilled water.

2.2. Sample preparation

Preparation of PVA/Starch and PVA/Starch/MMT blend films

PVA/Starch blend films were prepared using a solvent casting method. 1g Starch was dispersed in 20 mL distilled water at 95 ^{0}C for 30 min and, while stirring, starch gelatinization was induced. 1g PVA was dispersed in distilled water (30mL) and maintained at 90 ^{0}C for 30 min with continuous stirring until complete dissolution. For PVA blends, PVA/Starch was incorporated into the previously gelatinized starch dispersion by using Starch: PVA ratio of 1:1. Afterwards, Glycerol was added, as plasticizer, at a starch: glycerol ratio of 1:0.25, on the basis of previous studies. The mixture was stirred continuously for 30 min on a mechanical stirrer (1000 rpm) at room temperature. Bubbles formed during the preparation of blend films were removed by using a vacuum oven. The suspensions formed were poured onto Petri Dish plate to prepare blend film. The blend films were dried at room temperature for 72 h. For Starch/PVA/MMT blends, MMT with 5, 10 and 15 (w/w) ratios dispersed in 15 mL distilled water by sonication for 30 min at room temperature. Then, PVA, starch and MMT solutions were mixed together and stirred with a magnetic bar at 75 °C for 90 min. The suspension was poured in a Petri Dish plate and dried at room temperature for 72 h. Figure 1 shows the nanocomposite composed.

2.3. Characterizations

Thermogravimetric analysis was performed using a TGA from Polymer Laboratories (PL) model 1500. These analyses were examined with 6 ± 0.3 mg samples in platinum pans. Thermal degradation of samples was studied under nitrogen atmosphere. Experiments were performed at heating rates of 5, 10, 15, and 20 K min^{-1} from ambient temperature to 900 K, while the loss of mass was monitored. The morphology of the surface of the films was investigated using a field emission scanning electronic microscope (FESEM) of Mira 3-XMU type. The dried samples were coated with gold, and then photographed. Dynamic mechanical properties of the produced materials were measured using a DMA-TRITON model Tritec 2000 DMA operated in the three point bending horizontal measuring option. The DMTA tests experimental conditions were: temperature range, -50–150 ◦C; dynamic force, 700mN; static force, 750mN; and heating rate 5 ◦C/min. The frequency value used in the all cases was 1 Hz.

3. RESULTS AND DISCUSSION

3.1. Thermal stability of nanocomposites

Thermogravimetric analysis (TGA) has been commonly used to evaluate the thermal stability of polymer and their nanocomposites. In this technique, the weight loss of the

material due to the formation of volatile compounds under degradation because of the heating and temperature rising is monitored. The TGA technique is also used for studying the kinetics of thermal degradation [39–41]. The TGA data were prepared at four different heating rates, 5, 10, 15 and 20 °C/min. Figure 2 exhibits the weight loss percentage against temperature at heating rate 10 for the PVA/starch blend and Starch/PVA/MMT nanocomposites with diferent percentages of nano clay.

For better comparison between these curves, $T_{initial}$ (at 5 wt% loss), T_{max} (at 95 wt% loss), and the residual weight at 600 °C ($W_{residual}$) of the corresponding studied systems are listed in Table 2. According to the obtained results, the values of $T_{initial}$ and T_{max} increased by increasing the heating rate while the char yield decreased. Also the onset temperature of the degradation is about 10-30 ^{0}C higher for the nanocomposites than PVA/Starch blend. In all cases, the samples were not completely vaporized, and residue remained in the aluminum sample pans at the end of experiment. Thermal stability of the PVA/Starch/clay nanocomposites could be ordered as follows:

PVA/Starch <PVA/ Starch/Nano clay 15% < PVA/ Starch/Nano clay 5 %< PVA/ Starch/Nano clay 10%

Figure 3 shows DTG curves at 10 K min^{-1} heating rate for the blend and nanocomposites with various wt% of clay. Thermal degradation of polymers is related to the fact that the organic macromolecules inside the polymer matrix as well as low-molecular weight organic molecules are stable only up to a certain temperature range. The DTG curves (Figure 3) are very complex, samples exhibited a four-step degradation pattern and each of them shows some peculiarities. The first mass loss (2%) which appears as small signal temperatures below 90 ◦C is attributed to the elimination of absorbed/adsorbed water (physical dehydration process) from the studied materials. The second mass loss which appears below 220 ◦C (about 14%), represent the volatilization of the easily degraded components such as glycerol. The third step in the temperature range of 260-360 °C was related to the degradation of the starch/PVA blend. This step is followed by a further small mass loss up to 440 ^{0}C. After that, further heating broke down the polymer backbone and the TG/DTG curves presented a mass loss under air atmosphere for PVA/Starch blend and starch/PVA/MMT nanocomposites. After 600 ^{0}C, the main products were mainly the inorganic residues (i.e., Al2O3, MgO, and SiO2). Fig. 4 shows possible hydrogen bond formation between starch and PVOH Poly (vinyl alcohol).

Figure 5 and 6 show conversion (α) curve versus temperature and time for different percentages of nanoclay at the heating rate of 10 C/min, respectively. As expected, with increasing the percentage of nanoclay the conversion value occurred at a shorter temperature and time.

Figure 7a and 7b shows the degradation rate versus conversion at different

percentages of nanoclay and heating rate, respectively. It can be seen that the degradation rate is promoted by higher values of nanoclay as expected, and as the scan rate is raised the rate of degradation versus conversions level noticeably increases. It is clear that for each one there are ups and downs. It is obvious to see that the degradation rate of the nanocomposite reached a maximum between α=0.3 and α=0.65.

3.2. Degradation kinetics:

The activation energy (Eα) is the minimum energy required to initiate the thermal degradation process, and is related to the temperature dependence of the rate of degradation. The thermal degradation process for polymers may include several steps with different activation energies. Therefore, the overall degradation rate changes with temperature and the extent of degradation depends on the contribution of each step. Indeed, the efficient activation energy is a function of temperature and extent of degradation.

The Kissinger method was used to calculate the activation energy at different conversions by plotting ln (β/T^2) against 1/T (Figure 8). This method is based on a simple relationship between the activation energy and the heating rate. Using the Kissinger method, the value of activation energy obtained for pure PVA/St and PVA/St/Nano clay films were 172.20 and 225.70 Kj/mol, respectively. By using equation 10 (Ozawa method), the activation energy of degradation can be obtained from the plot of log[β] vs. 1/T. Fig. 9 shows these plots between log β and 1/T at different conversion values for pure PVA/St and PVA/St/Nano clay samples, and the value of activation energy obtained for pure PVA/St and PVA/St/Nano clay films were 125.06 and 154.53 Kj/mol, respectively. According to the results, we can find the consistency of activation energy obtained from Kissinger and Flynn-Wall-Ozawa methods. The advantage of both models was that they could be employed without any knowledge about the reaction mechanism.

The advanced isoconversional method was used to acquire different activation energies as a function of the extent of degradation. The dependence of the apparent activation energy (Ea) on the extent of conversion (α) for non-isothermal degradation of the PVA/Starch blend and PVA/Starch/Nanoclay Nanocomposites was appraised from the straight line slope of the corresponding Friedman's isoconversional method (Eq. 9). Figure 10 illustrates the relationship between the activation energy Ea and the degree of conversion (α). At a given extent of degradation, the nanocomposites samples present about 20-40 kJ mol^{-1} higher than that of the PVA/Starch sample. In the present case, situation is much complicated because the clay could interact with the two components (PVA and starch). The activation energy for the PVA/Starch blend and PVA/ Starch/Nanoclay increased irregularly between α = 0.05-0.5 and then

increased to α = 0.95 on a regular basis.

Figure 10 show that the presence of nano clay in the neat blend increases the degradation activation energy. It is commonly known that the thermal degradation is initiated in weak link sites and thus the activation energy for earlier stages was lower. As shown in Fig. 10, the activation energy sometimes shows a fast drop. It is at the point of transition from one mass loss step to another. According to the results, we can find the consistency of activation energy of Kissinger, Flynn-Wall-Ozawa and Friedman methods for PVA/ starch and PVA/ starch /MMT blends. This means that these methods are suitable and effective for degradation of PVA/ starch and PVA/ starch /MMT blends. The results of the three methods are shown in Table 3.

Invariant kinetic parameters (IKP) method requires several α−*T* curves recorded at different heating rates and this method gives values of E_{inv} and A_{inv}, which correspond to the true kinetic model that describes the investigated process at all heating rates. Figures 11 show variation of lnA with E_a using IKP method for (a) pure and (b) Nanocomposite and the results are summarized in Table 4.

3.3. Master plots based on the differential form of the kinetic equation:

Once the apparent activation energy has been determined, it is possible to find the kinetic model which corresponds to the better description of the experimental data. Using a reference point at a = 0.5, the following equation could be derived from Eq. 6:

$$\frac{f(\alpha)}{f(0.5)} = \frac{(\frac{d\alpha}{dT})}{(\frac{d\alpha}{dT})0.5} \frac{EXP(\frac{E_\alpha}{RT})}{EXP(\frac{E_\alpha}{RT0.5})} \quad (13)$$

Where $(da/dt)_{0.5}$, $T_{0.5}$ and $f(0.5)$ are the degradation rate, the degradation temperature, and the differential function of the reaction model at a = 0.5, respectively. The left-hand side of Eq. (13) is a reduced theoretical curve, which is characteristic of each kinetic function. The right-hand side of the equation is associated with the reduced rate and can be obtained from the experimental data if the apparent activation energy is known. The accuracy of the selected model was checked by producing master curves of f (α) versus α % for different mechanisms.

Figure 12 shows the theoretical and experimental differential curves established using Eq. (13) at 10 K min^{-1}. The comparison of the experimental master plots with theoretical ones indicates that the kinetic process of PVA/St thermal degradation can be most probably described by A_2 model, $[-\ln (1-\alpha)]^{1/2}$, and for PVA/St/Nano clay nanocomposite can be most probably described by A_3 model, [-ln

$(1-\alpha)]^{1/3}$. The physical description of the A2, A3 mechanism is Nucleation and growth.

4. SOIL BURIAL DEGRADATION:

Soil burial degradation was carried out to study the degradation of the nanocomposite films under natural environmental conditions. Figure 13 show Weight loss (%) of films after burial in soil for 120 days. It is obvious after burying the films in the soil, the size of the films reduced and the surface of films became hard and fragile. The results showed that PVA/Starch sample has higher weight loss (33 % after 14 weeks) in comparison with PVA/Starch/Nanoclay and PVA/Starch/glutaraldehyde samples which can be due to the ability of the starch to absorb higher amount of moisture. The water absorbed by the films caused the films to swell and allowed the microbes to growth on the surface of the films. It is observed from the figure that percent weight loss of all the samples increase continuously with increase in the number of days. The crosslinked PVA/St and PVA/St/nanoclay films showed lower weight loss as compared to PVA/St film due to the decrease in hydrophobicity of the films after cross linking and as a result of the addition of nanoclay, respectively.

5. SCANNING ELECTRON MICROSCOPY (SEM)

To get insights about the morphology of the produced nanocomposite, FESEM was used. Microstructures of the fractured cross-section of PVA/Starch with and without MMT are shown in Fig. 14 (a,b) at various magnifications. White zones in the images (a) correspond to the MMT. The different shape and size of the MMT in the PVA/Starch matrix may be attributed to various condensation patterns during the network build-up. However, a relatively good adhesion was observed between PVA/Starch matrix and MMT at 10 wt.%.

6. Dynamic mechanical thermal analysis

The visco-elastic properties of PVA/starch blend and PVA/starch / MMT nanocomposite were studied by dynamic mechanical analysis. Dynamic mechanical analysis is useful to evaluate the performance of materials under stress and temperature. In this study, Young's modulus is defined as the measure between applied stresses and the resulting strain per unit length and the tanδ is the ratio of the loss modulus to the storage modulus E□/E□.

The variation of the storage modulus and tanδ for PVA/starch blend and PVA/Starch / MMT nanocomposite as a function of time and temperature is shown in Fig. 15 (a, b) respectively. In these figures the rise time, the temperature increases. At

low temperature, storage modulus values of PVA/starch and nanocomposite are close, but at higher temperature storage modulus has fallen and it are higher for nanocomposites than the system PVA/ST blend. Because, at low temperature nanoclay do not contribute much too imparting stiffness to the material, but on increasing the temperature the drop of matrix modulus is by the fibre stiffness. In fact, the addition of nanoclay to system to cause more stress on the interface. As figure is shown, the tanδ was high for the system PVA/ST blend due to the high diminution of the storage modulus values on increasing the temperature. Also for the present study the glass transition temperature can determine by the maximum of the tan δ versus temperature curve. So it can be concluded that the addition of nanoclay improved mechanical properties of nanocomposites.

4. CONCLUSIONS

In this study we evaluated the starch/PVA blend and starch/PVA/MMT nanocomposite were synthesized and their thermal stability studied by non-isothermal thermogravimetric analysis. Model-free isoconversional methods of Kissinger–Akahira–Sunosen, Flynn–Wall–Ozawa and Friedman were also used to analyze the conversion dependence of the global activation energy, Ea. The activation energy values obtained by the methods showed that these three methods were suitable to describe the thermal degradation of starch/PVA blend and starch/PVA/MMT nanocomposite. The results obtained from the method chosen in this study suggested that PVA/Starch with 10 wt% MMT has best thermal stability because has higher activation energy. By comparing the master plots corresponding to the different kinetic models with the plots relating to the f(α) function versus conversion, the kinetic functions for thermal degradation of the starch/PVA blend and starch/PVA/MMT nanocomposite were evaluated to be A2 and A3, respectively.

The results from DMTA measurements were showed incorporation of the MMT into blend and improved the mechanical properties of the produced nanocomposite in terms of modulus increment. From the SEM figure, it can be concluded that MMT disperse well in the PVA/Starch matrix. This dispersion is useful to improve the mechanical properties of the film and shows an agreement with the mechanical property results. Also, the biodegradation of PVA/S blend films was studied by burial in soil and the results showed that the Starch has a high moisture absorption capacity and therefore the first weeks is associated with high mass reduction.

DISCLOSURE STATEMENT

No potential conflict of interest was reported by the authors.

Finding

The financial support from University of Mazandaran is gratefully acknowledged.

References

[1] Ray, S. S, M. Okamoto. (2003). Polymer/layered silicate nanocomposites: A review from preparation to processing. Progress in Polymer Science, 28(11):1539–1641.

[2] Alexandre, M., P. Dubois. (2000). Polymer-layered silicate nanocomposites: Preparation, properties and uses of a new class of materials. Materials Science and Engineering R-reports, 28(1): 1–63.

[3] Okada, A.; Usuki, A. (2006). Macromol. Mater. Eng, 291, 1449−1476.

[4] Alexandre, M.; Dubois, P. Mater. Sci. Eng. R, 28, 1−63.

[5] Sudhakara, P.; Kannan, P.; Obireddy, K.; Rajulu, A. V. (2000). J. Mater. Sci. 46, 2778−2788.

[6] Zanetti, M.; Lomakin, S.; Camino, G. (2000). Macromol. Mater. Eng. 279, 1−9.

[7] Manias, E.; Touny, A.; Wu, L.; Strawhecker, K.; Lu, B.; Chung, T. C. (2001). Chem. Mater. 13, 3516−3523

[8] Tjong, S. C. (2006). Mater. Sci. Eng. R, 53, 73−197.

[9] Krishna, S. V.; Pugazhenthi, G. (2011). J. Appl. Polym. Sci. 120, 1322−1336.

[10] Morales-Gamez, L.; Franco, L.; Puiggali. (2011). J. Thermochim. Acta 512, 142−149.

[11] Ray, S. S.; Okamoto, M. (2003). Prog. Polym. Sci. 28, 1539−1641.

[12] Pavlidou, S.; Papaspyrides, C. D. (2008). Prog. Polym. Sci. 33, 1119−1198.

[13] Ramaraj, B. (2007). Crosslinked poly(vinyl alcohol) and starch composite films. II.Physicomechanical, thermal properties and swelling studies. Journal of Applied Polymer Science, 103, 909, 916.

[14] Cano, A., Fortunati, E. L. E. N. A., Cháfer, M., Kenny, J. M., Chiralt, A., & González-Martínez, C. (2015). Properties and ageing behaviour of pea starch films as affected by blend with poly (vinyl alcohol). *Food Hydrocolloids*, *48*, 84-93.

[15] Jim_enez, A., Fabra, M. J., Talens, P., & Chiralt, A. (2012a). Edible and biodegradable starch films: a review. Food and Bioprocess Technology, 5(6), 2058e2076.

[16] Aydın, A. A., & Ilberg, V. (2016). Effect of different polyol-based plasticizers on thermal properties of polyvinyl alcohol: starch blends. *Carbohydrate Polymers*, *136*, 441-448.

[17] Azahari, N. A., Othman, N., & Ismail, H. (2011). Biodegradation studies of polyvinyl alcohol/corn starch blend films in solid and solution media. *Journal of physical science*, *22*(2), 15-31.

[18] Tang, X., & Alavi, S. (2011). Recent advances in starch, polyvinyl alcohol

based polymer blends, nanocomposites and their biodegradability. *Carbohydrate Polymers*, *85*(1), 7-16.

[19] Ramaraj, B. (2007). Crosslinked poly (vinyl alcohol) and starch composite films: Study of their physicomechanical, thermal, and swelling properties. *Journal of applied polymer science*, *103*(2), 1127-1132.

[20] Nistor, M. T., & Vasile, C. (2013). Influence of the nanoparticle type on the thermal decomposition of the green starch/poly (vinyl alcohol)/montmorillonite nanocomposites. *Journal of thermal analysis and calorimetry*, *111*(3), 1903-1919.

[21] Ali SS, Tang X, Alavi S, Faubion J. (2011). Structure and physical properties of starch/poly vinyl alcohol/sodium montmorillonite nanocomposite films. J Agric Food Chem, 59(23), 12384–95.

[22] Tang X, Alavi S. (2011). Recent advances in starch, polyvinyl alcohol based polymer blends, nanocomposites and their biodegradability. *Carbohydrate polymers*, 85, 7–16.

[23] Cinelli P, Chellini E, Gordon SH, Imam SH. (2003). Characteristics and degradation of hybrid composite films prepared from PVA, starch and lignocellulosics. Macromol Symp, 197,143–56.

[24] Sadhu, S. D., Soni, A., & Garg, M. (2015). Thermal Studies of the Starch and Polyvinyl Alcohol based Film and its Nano Composites. *J Nanomedic Nanotechnol S*, *7*, 2.

[25] Vyazovkin, S., I. Dranka, X. Fan, R. Advincula, 2004. Kinetics of the thermal and thermo-oxidative degradation of a polystyrene–clay nanocomposite. Macromolecular Rapid Communications, 25: 498-503.

[26] Fakhrpour, G., Bagheri, S., Golriz, M., Shekari, M., Omrani, A., & Shameli, A. (2016). Degradation kinetics of PET/PEN blend nanocomposites using differential isoconversional and differential master plot approaches. *Journal of Thermal Analysis and Calorimetry*, *124*(2), 917-924.

[27] Erceg, M., Kovačić, T., & Perinović, S. (2008). Kinetic analysis of the non-isothermal degradation of poly (3-hydroxybutyrate) nanocomposites. *Thermochimica Acta*, *476*(1), 44 50.

[28] J.H. Flynn, L.A.Wall, J. Res. Natl. Bur. Stand. 70A (1966) 487–523.

[29] T. Ozawa, Bull. Chem. Soc. Jpn. 38 (1965) 1881–1889.

[30] H.E. Kissinger, Anal. Chem. 29 (1957) 1702–1706.

[31] T. Akahira, T. Sunose, Res. Report Chiba Inst. Technol. 16 (1971) 22–31.

[32] Taghizadeh, M. T., Yeganeh, N., & Rezaei, M. (2014). Kinetic analysis of the complex process of poly (vinyl alcohol) pyrolysis using a new coupled peak deconvolution method. *Journal of Thermal Analysis and Calorimetry*, *118*(3), 1733-1746.

[33] Slopiecka, K., Bartocci, P., & Fantozzi, F. (2012). Thermogravimetric analysis and kinetic study of poplar wood pyrolysis. *Applied Energy*, *97*, 491-497.

[34] Friedman, H. L. (1964, January). Kinetics of thermal degradation of char-forming plastics from thermogravimetry. Application to a phenolic plastic. In *Journal of Polymer Science: Polymer Symposia* (Vol. 6, No. 1, pp. 183-195). Wiley Subscription Services, Inc., A Wiley Company.

[35] Li, S. D., Li, P. W., Yang, Z. M., Dong, J. J., Yang, X. H., & Yang, L. (2014). Thermal degradation of hydroxypropyl trimethyl ammonium chloride chitosan–Cd complexes. *Journal of Thermal Analysis and Calorimetry*, *118*(1), 15-21.

[36] P. Budrugeac, E. Segal, Int. J. Chem. Kin. 33 (2001) 564–573.

[37] Janković, B., Stopić, S., Bogović, J., & Friedrich, B. (2014). Kinetic and thermodynamic investigations of non-isothermal decomposition process of a commercial silver nitrate in an argon atmosphere used as the precursors for ultrasonic spray pyrolysis (USP): The mechanistic approach. *Chemical Engineering and Processing: Process Intensification*, *82*, 71-87.

[38] Burnham, A. K. (2017). Introduction to Chemical Kinetics. In *Global Chemical Kinetics of Fossil Fuels*. Springer International Publishing. 25-74.

[39] A. Aboulkas, K. El Harfi, A. El Bouadili. (2008). Energy Convers. Manage, 49, 71.

[40] L. Zhou, T. Luo, Q. Huang. (2009). Energy Convers. Manage, 50, 705.

[41] Y. Zhaosheng, M. Xiaoqian, L. Ao. (2009). Energy Convers. Manage. 50, 561.

Table 1. Kinetic models with symbols and conversion function, f (α)

Kinetic model	Symbol	$f(x)$
n-order		
First order	F_1	1-α
Second order	F_2	$(1- \alpha)^2$
Third order	F_3	$(1- \alpha)^3$
*n*th order	F_n	$(1- \alpha)^4$
Deceleratory α-time		
1. Diffusion		
1. D diffusion	D_1	$1/(2\ \alpha)$
2. D diffusion	D_2	$[-\ln(1-\alpha)]^{-1}$
3. D diffusion-Jander	D_3	$\frac{3}{2}(1-\alpha)^{2/3}/\ 2[1-(1-\alpha)^{1/3}]$
3. D diffusion - Ginstling rounshtein	D_4	$3/2[(1- \alpha)^{1/3} -1]$
2. Phase boundary		
Contracting area	R_2	$2(1- \alpha)^{1/2}$
Contracting volume	R_3	$3(1- \alpha)^{2/3}$
Nucleation (Avrami – Erofeev)		
Two- dimensional nucleation	A_2	$2\ (1- \alpha)\ [-\ln\ (1- \alpha)]^{1/2}$
Three- dimensional nucleation	A_3	$3\ (1- \alpha)\ [-\ln\ (1- \alpha)]^{2/3}$
Four- dimensional nucleation	A_4	$4\ (1- \alpha)\ [-\ln\ (1- \alpha)]^{3/4}$
n- dimensional nucleation	A_n	$n\ (1- \alpha)\ [-\ln\ (1- \alpha)]^{(n-1)/n}$

Table 2. TGA data of the thermal degradation at different heating rates

β (°C/min)	PVA/Starch	PVA/Starch/MMT (5%)	PVA/Starch/MMT (10%)	PVA/Starch/MMT (15%)
5	T_i((^{0}C) =66	T_i((^{0}C) =92	T_i(^{0}C)=85	T_i(^{0}C) =76
	T_{max}(^{0}C) =60	T_{max}(^{0}C) =605	T_{max}(^{0}C) =605	T_{max}(^{0}C) =605
	W_{red}=8.44	W_{red}=9.06	W_{red}=12.66	W_{red}=17.01
10	T_i(^{0}C) = 95	T_i(^{0}C) =108	T_i(^{0}C) =115	T_i(^{0}C) =117
	T_{max}(^{0}C)=605	T_{max}(^{0}C) =607	T_{max}(^{0}C)=606	T_{max}(^{0}C) =607
	W_{red}=8.20	W_{red}=7.46	W_{red}=12.52	W_{red}=16.54
15	T_i(^{0}C)=98	T_i(^{0}C) =120	T_i(^{0}C) =117	T_i(^{0}C) =117
	T_{max}(^{0}C)=606	T_{max}(^{0}C) =606	T_{max}(^{0}C) =607	T_{max}(^{0}C) =604
	W_{red}=8.04	W_{red}=7.68	W_{red}=12.25	W_{red}=16.07
20	T_i(^{0}C) =102	T_i(^{0}C) =130	T_i(^{0}C) =131	T_i(^{0}C) =114
	T_{max}(^{0}C)=607	T_{max}(^{0}C) =606	T_{max}(^{0}C) =608	T_{max}(^{0}C) =608
	W_{red}=7.06	W_{red}=6.85	W_{red}=11.63	W_{red}=15.09

Table 3. The activation energy and rate constants for three different methods

Samples	Ea(Kj/mol) KSA	Ea(Kj/mol) OWZ	Ea(Kj/mol) FR	K(min^{-1})
PVA/Starch	133.17	125.06	141.55	0.0082
PVA/Starch/MMT (5%)	153.92	148.76	183.23	0.0087
PVA/Starch/MMT (10%)	162.84	154.53	191.40	0.0085
PVA/Starch/MMT (15%)	145.97	137.77	165.83	0.0088

Table 4: True values of ln *A,* a* *and* b*corresponding to the calculated IKP method.

	lnA	a*	b*
Neat PVA/st	60	0.42	14.71
Nnocomposite	65	0.36	15.45

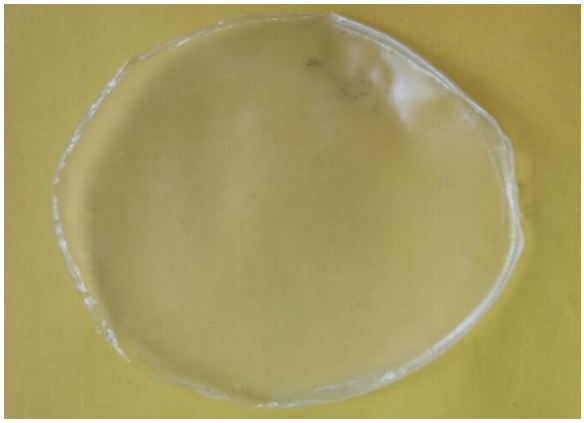

Figure 1. Film of Sample PVA/Starch/MM

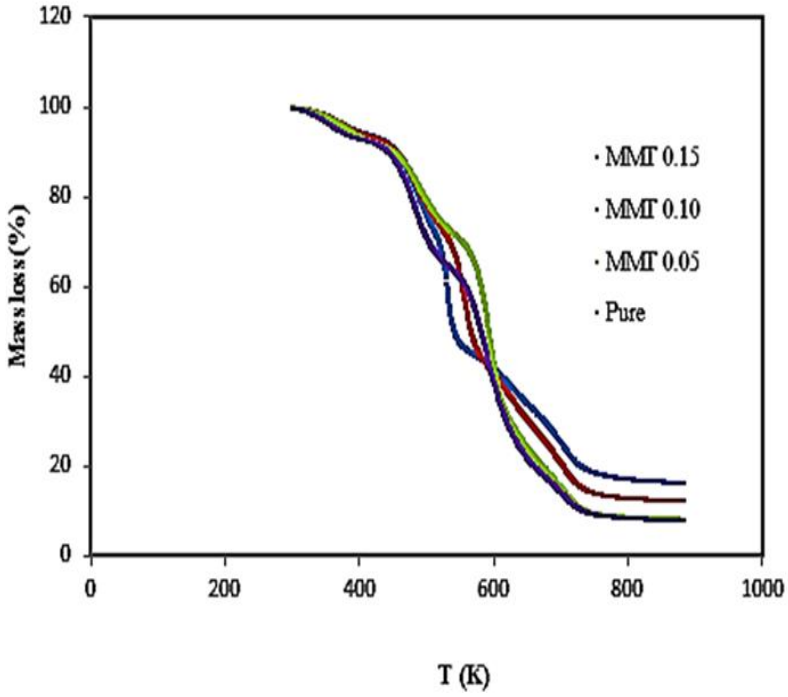

Figure 2. TGA curves of the PVA/St and PVA/St/MMT films

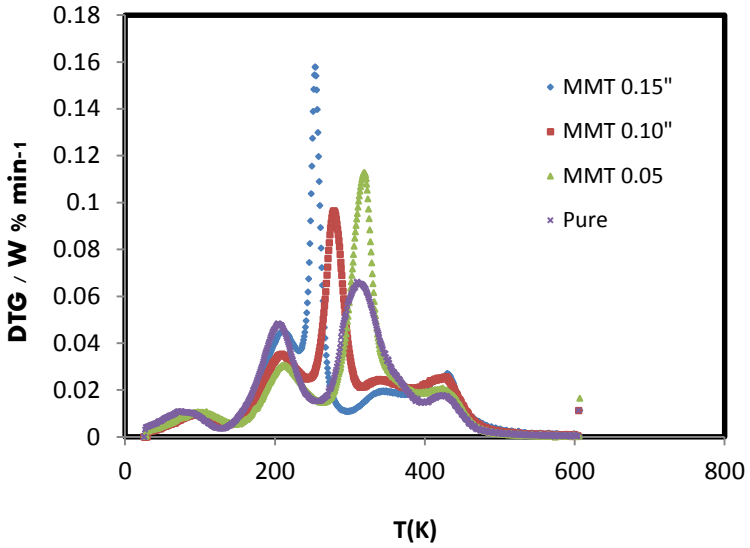

Figure 3. DTG curves of the PVA/ST and PVA/ST/MMT films

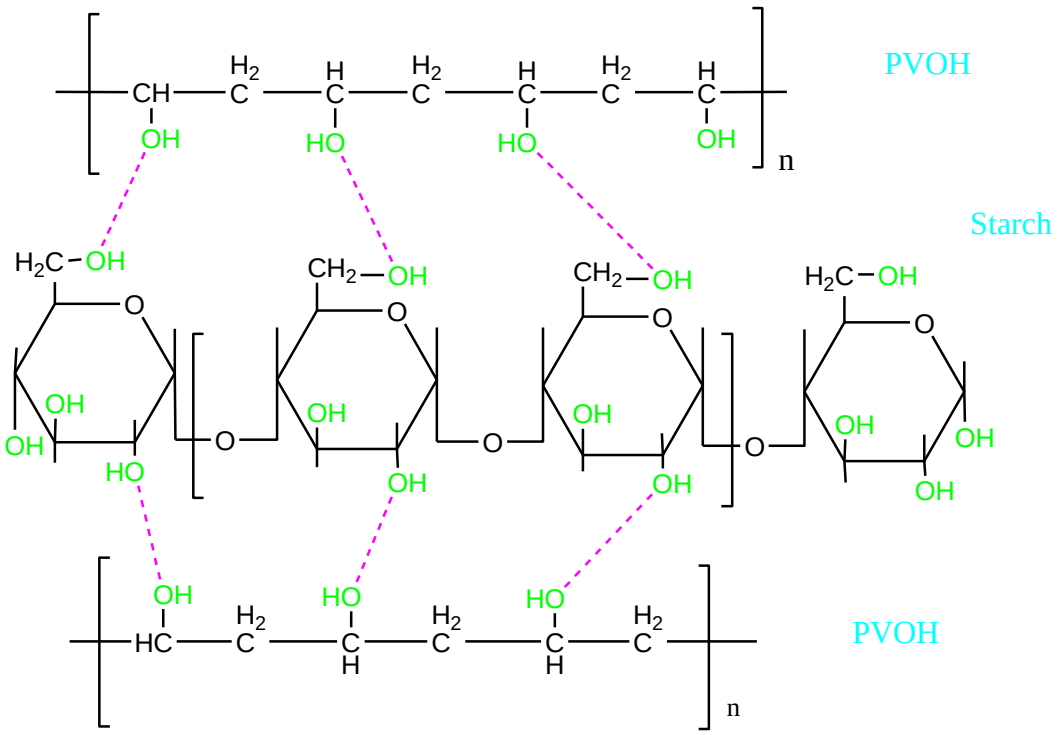

Figure 4. Possible hydrogen bond formation between starch and PVOH.

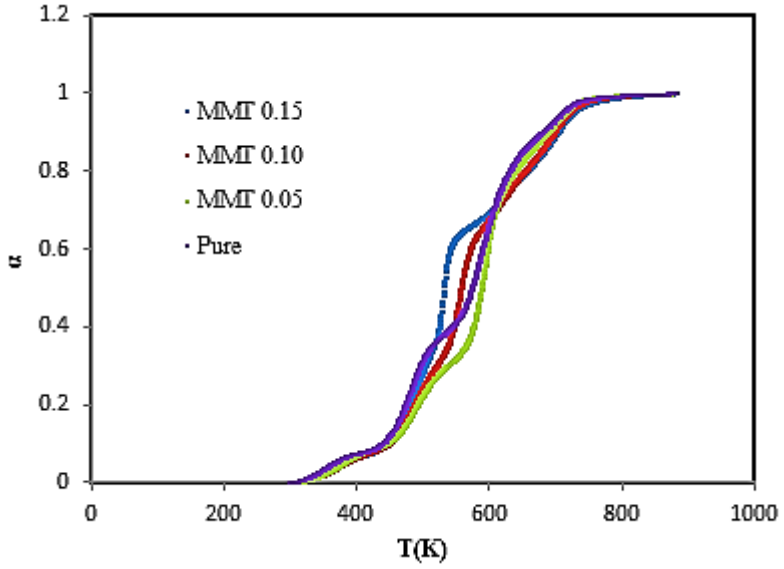

Figure 5. Degree of conversion ersus temperature plots at various percentages of nano clays

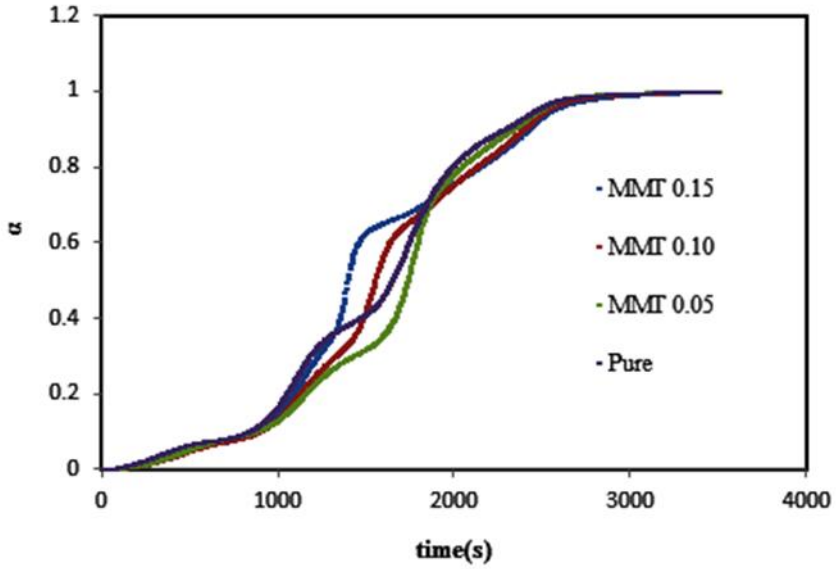

Figure 6. Degree of conversion versus time plots at various percentages of nano clays

(a)

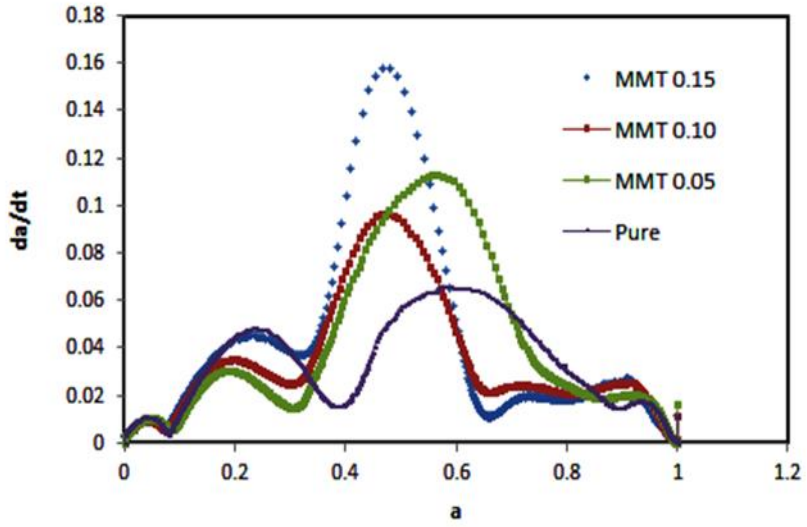

(b)

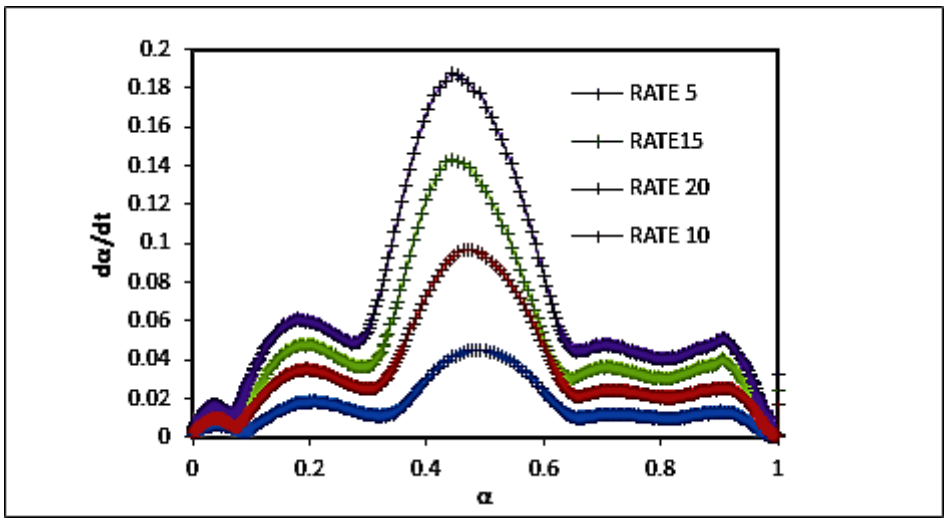

Figure 7. Reaction rate versus conversion plots at various percentages of nano clays (a) and various scan rate (b)

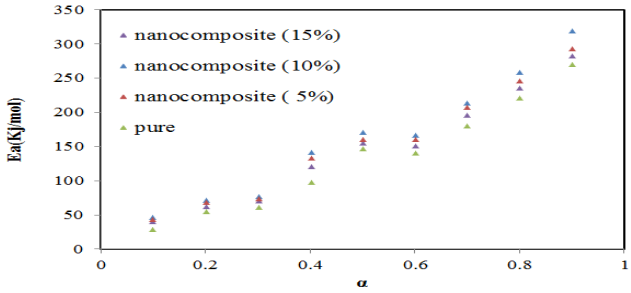

Figure 8. Kissinger plots for the PVA/ST and PVA/ST/MMT films

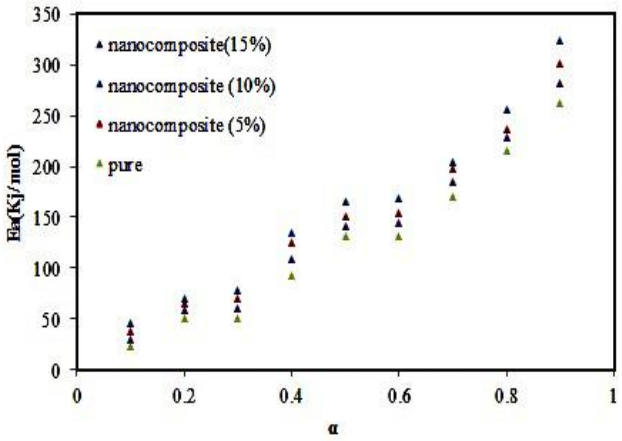

Figure 9. Ozawa plots for the PVA/ST and PVA/ST/MMT films

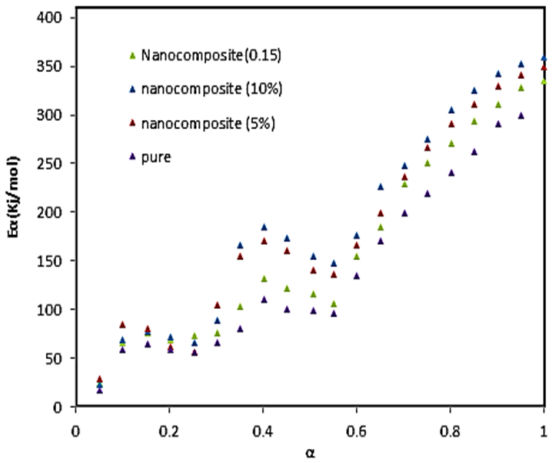

Figure 10. Variation of effective activation energy *Ea* with conversion *α* during the thermal degradation using advanced isoconversional method.

(a)

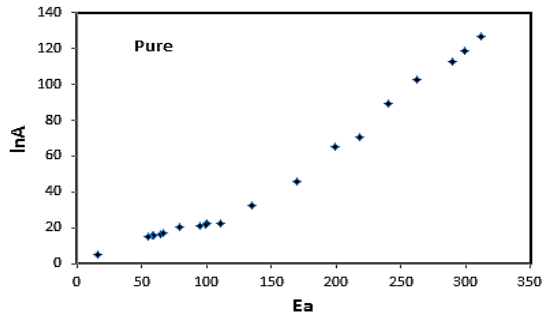

(b)

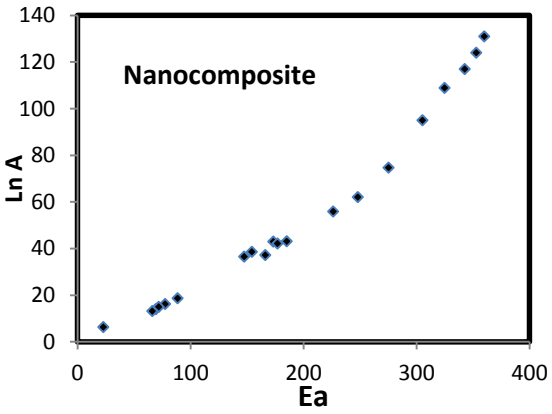

Figure 11. Variation of lnA with E_a using IKP method. (a) neat PVA/St (b) Nanocomposite

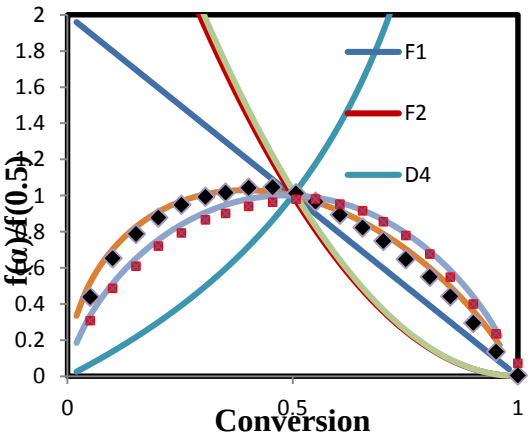

Figure 12. Comparison of master curve plots corresponding to different models.

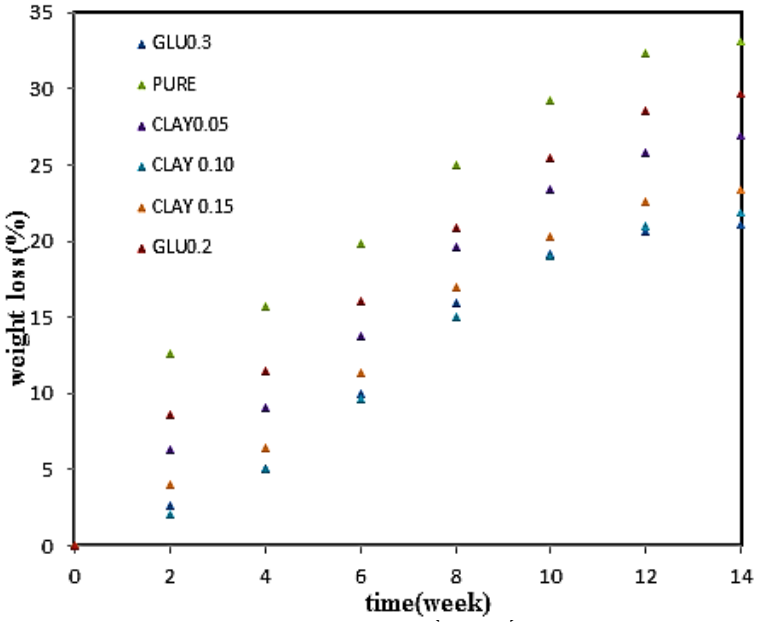

Figure 13. Biodegradability of PVA/St films, cross linked PVA/St films and PVA/St/MMT films

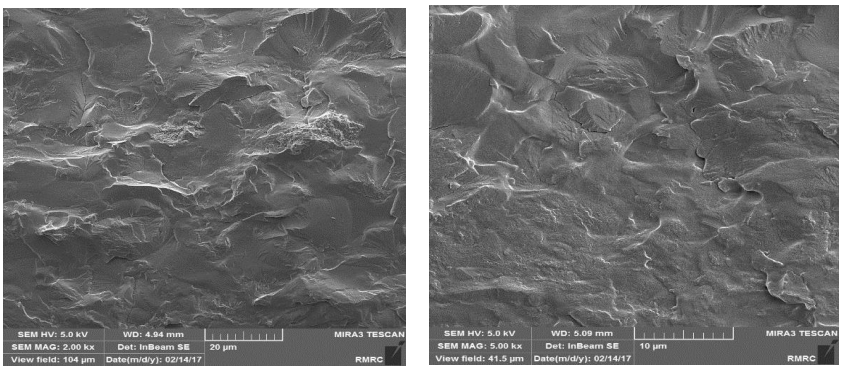

(a) (b)

Figure14. FESEM micrographs of the fracture surfaces of (a) nanocomposite , (b) neat PVA/St

(a)

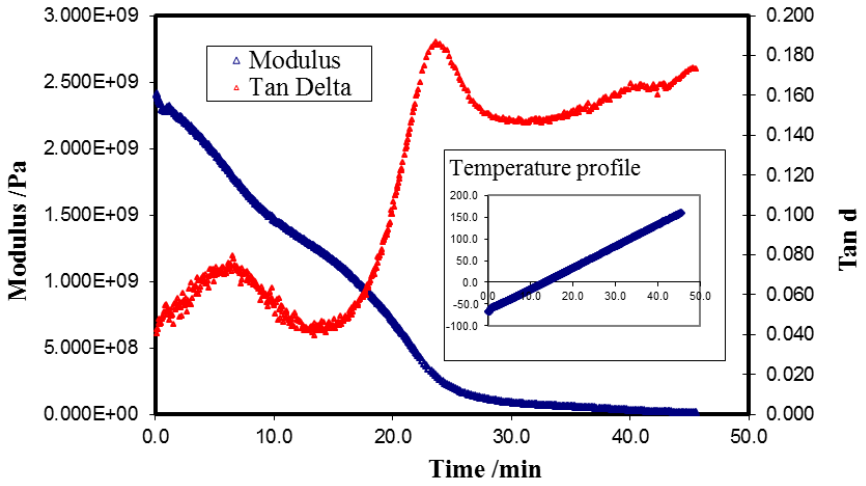

(b)

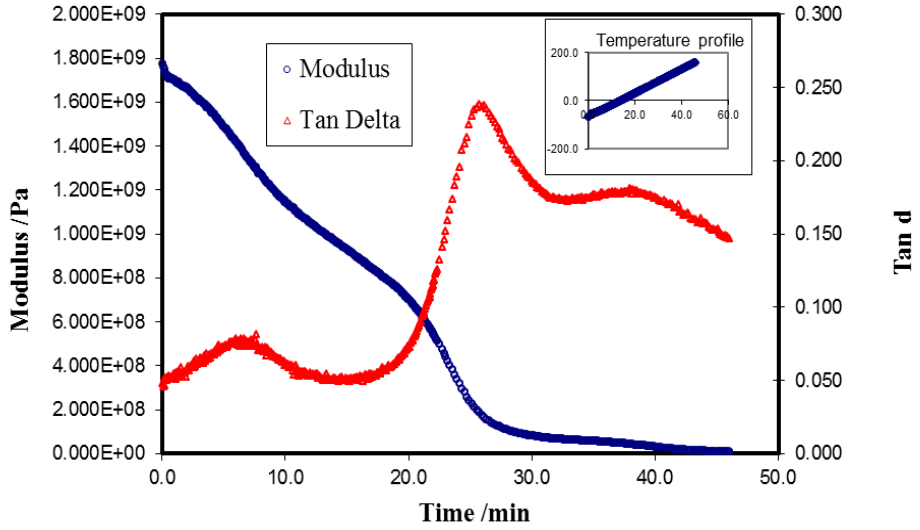

Figure 15. Curves of tan δ and modulus versus time and temperature of the (a) nanocomposite , (b) neat PVA/St